Investigation of Electro-Mechanical Fuel System of AGT-1500 Gas Turbine Engine

Omar Salah and Islam Nasser

Department of Mechanical Engineering, Military Technical College, Cairo, 11766, Egypt
omarsalahomar555@gmail.com, jrnaser4@gmail.com

Supervisor: Assoc. Prof. Dr. Mohamed Atef Kamel
Department of Mechanical Engineering, Military Technical College, Cairo, 11766, Egypt,
mohamed.atef.kamel@mtc.edu.eg

Abstract— The fuel flowrate and air flow direction are the main parameters affecting the gas turbine engine performance. The fuel management system is a full authority digital electronic computing control system. It positions the inlet guide vanes (IGV), power turbine stators (PTS) and meters fuel flow to the engine through fuel metering system (FMS) to obtain optimum performance. The system consists of two control units that must work in conjunction with each other. These units are the electro-mechanical fuel system (EMFS) and the digital electronic control unit (DECU). One of the most important and challenging concerns of engine design and control is driving a valid model for the EMFS with its three subsystems. Physics-based, black box and grey box models are used in driving a model for any system. In this paper a physics-based model for IGV and PTS systems have been estimated and validated using SIMULINK. As it is very hard to model the electrohydraulic FMS because of its complicity and integrity. It is preferred to treat the system as a black box. So, a model for an electrohydraulic FMS has been estimated and validated using MATLAB system identification toolbox (SIT). The driven model has been validated using a different measured data set to insure a good representation of the physical system. Results show that the obtained model follows the real system with good accuracy.

Index Terms— Gas turbine engine, Hydraulic control, Electro-mechanical fuel system, Inlet guide vanes , power turbine stator, fuel metering system.

I. Introduction

Engines start was not only prior 1860s but it even started before 350 BCE with the fire piston, the first device to exploit compression-ignition. Ever since, engines have been developing to overcome the facing problems and to improve their performance reaching petrol and diesel engines. After World War II, it was clear that gas turbine engine had a big advantage over both engines for its lower weight, less noise, less smoke emissions, greater power and mechanical efficiency. Us ing en gines power instead of steam power used in navy, pump stations and power generation gave the idea of using a gas turbine power plant in an armored land vehicle. In October 1965, the U.S. Army Tank Automotive Command (TACOM) awarded a contract for development of a tank turbine engine, The AGT1500 was designed by AVCO Lycoming (now Honeywell Defense and Space) to be the alternative power source for the diesel powered multinational Main Battle Tank (MBT) 70 tank.

Jet engine controllers have changed in two main areas, their hardware and the concept of control. They have been investigated in many studies, The historical progress of the development of gas turbine engine controllers' hardware could be divided into five main categories:

- Hydro-mechanical fuel controllers;
- Hydro-mechanical/Electronic Fuel Control;
- Digital Electronic Engine Control (DEEC);
- Full Authority Digital Electronic Control (FADEC);
- Advanced Engine Control.

The historical progress of the development of gas turbine engine (GTE) control systems could be divided into four phases: [1]

- Single-input single-output (SISO) control algorithm;
- Min–Max or cascade control algorithm;
- Advanced control algorithm;
- More electric and electronic control algorithm.

The investigated gas turbine engine is controlled with a full authority digital electronic computing control system.This system consists of two control units that must work in conjunction with each other. These units are the electro-mechanical fuel system (EMFS) and the digital electronic control unit (DECU).

In this paper we aim to build a complete dynamic model that can be used in the analysis of the system response and validate this model, in addition to build a controller for the system along all the working conditions.

The organization of the paper is

- section (2) : Methodology
- section (3) : System description
- section (4) : Mathematical Model
- section (5) : Control system
- section (6) : Exprimental work
- section (7) : Results
- section (8) : Conclusion
- section (9) : Future Work

II. Methodology

The methodology plan of the project is described as:

- Study the fuel supply system of M1A1 MBT, gas turbine engine AGT 1500 and its electro-mechanical fuel system (EMFS).
- Setting a test rig which will be responsible to be the reference to validate our dynamic model and controller.
- Measure all the influential parameters and dimensions identifying the system and affect its operation.
- Design a graphical user interface (GUI) using LabVIEW to display and log the system response to validate the mathematical model.
- Design a mathematical model which represent the actual system using SIMULINK.
- Comparing the measured and the predicted results for the open loop configuration and validate the system model.

III. System Description

The fuel management system is a full authority digital electronic computing control system. The system consists of two control units that must work in conjunction with one another. These units are:

- Electro-mechanical fuel system (EMFS)
- Digital electronic control unit (DECU).

These units are responsible of controlling main three subsystems as shown in figure 1, these subsystems are:

- Inlet Guide Vanes (IGV) subsystem.
- Power turbine stators (PTS) subsystem.
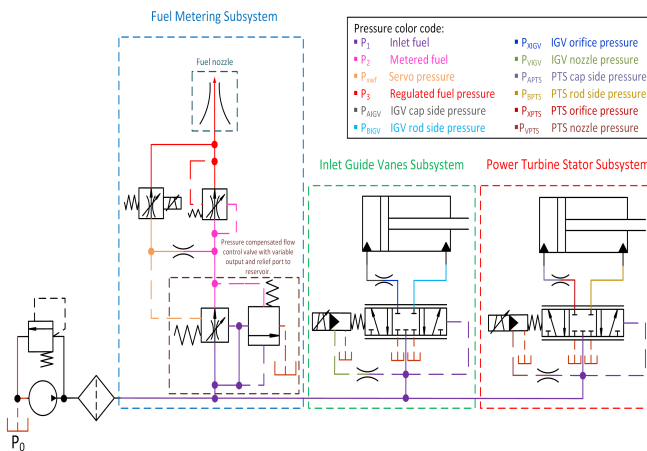- Fuel metering (FM) subsystem.

Fig. 1.   Electro-mechanical fuel system EMFS

A. Inlet Guide Vanes (IGV) subsystem

Inlet guide vanes (IGV) subsystem is a part of the fuel management and control system of AGT1500 gas turbine engine. It is considered as electro-hydraulic servo actuator system (EHSA) which accurately controls the inlet guide vanes of the engine. The subsystem has been built in three main parts, these parts are:

- Electro-magnetic proportional solenoid.
- Electro-hydraulic servo-proportional valve.
- Electro-hydraulic servo actuator.

Supply pump is used to supply the system with diesel fuel. In order to regulate the pump pressure at 9 bars, a pressure regulator valve is used. The regulated pressure is pumped into a directional control valve. The valve's spool location identifies the direction and the flow rate comes out from the valve to the actuator. The spool location is controlled by proportional solenoid in contactless manner.   hydraulic amplifier is in the valve spool. It is controlled by the gab separating the amplifier variable nozzle and the linear solenoid core. The change of the gap width leads to variable nozzle area which in turn changes the pressure on the upside of the spool. In the other side the supply pressure conducts a constant pressure force on the down side of the spool all the time. Different pressure forces on the upside and downside of the spool move the spool to maintain the gap width constant. The hydraulic amplifier works on converting the small solenoid core displacement into a considerable pressure force to move the spool.

-Electro-magnetic proportional solenoid.

The electro-magnetic proportional solenoid represented in this study is a linear traverse and limited travel DC solenoid.
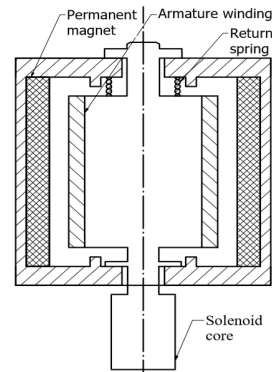

Fig. 2.   Electro-magnetic proportional solenoid

As shown in Figure 2, It consists of permanent magnet poles, armature coil, plunger core of iron and return spring.

When voltage (Vi) is applied to the coil, current (i) passes through it and creates a magneto motive force. This force acts against the magneto motive force of the permanent magnet and makes them repel.

-Electro-hydraulic servo-proportional valve.

As shown in Figure 3, The valve's spool inner bore acts as a hydraulic amplifier. It's excited by the small displacement of the solenoid core which changes the gap accordingly.The gap changes the amplifier pressure Pv, leads the spool to move as a reason of pressure differences to balance the gap in the equilibrium distance.
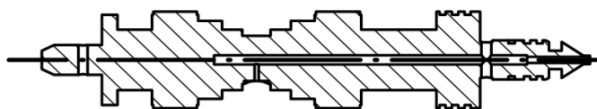

Fig. 3.   Electro-hydraulic servo-proportional valve

-Electro-hydraulic servo actuator.

The electrohydraulic valve controls the piston's movement both its direction and rate, in order to maintain accurate position control.

Fig. 4.   Electro-hydraulic servo actuator

B. Power turbine stators (PTS) subsystem

Power turbine stator PTS and inlet guide vanes IGV are almost 2 identical systems except the electro-hydraulic servo acruator.They are different in the dimensions as bore diameter, rod diameter and stroke.

C. Fuel metering (FM) subsystem

Fuel metering (FM) subsystem is a part of the fuel management and control system of AGT1500 gas turbine engine of M1A1 MBT. It is responsible of metering fuel flow to the engine to obtain optimum performance. The subsystem has been built in eight main parts which will not be explained in this study as we will study it as a black box, these parts are:
- Bypass valve.
- Pressurizing valve and fuel flow solenoid.
- Metering valve and LVDT.
- Relief valve and backup flow solenoid.
- Cutoff Solenoid.

IV. Mathematical Model

-Introduction.

A mathematical model is an abstract model that uses mathematical language to describe the behavior of a system. Mathematical models are used particularly in the natural sciences and engineering disciplines (such as physics, biology, and electrical engineering) but also in the social sciences (such as economics, sociology and political science); physicists, engineers, computer scientists, and economists use mathematical models most extensively. Mathematical models can take many forms, including but not limited to dynamical systems, statistical models, differential equations, or game theoretic model[2] . Physics-based, black box and grey box models are used in driving a model for any system.

A. IGV subsystem model

In order to describe the electro-hydraulic system under study, a physics based mathematical model has been driven. This model explains the behavior of system's (current, pressures, flow rates, and displacements of mechanical part) using the suitable equations for each phenomenon which are mentioned in another thesis[3] and modified to suit our system as shown in figure 5.
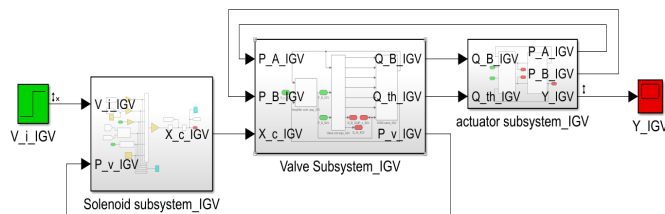

Fig. 5.   IGV total system

B. PTS subsystem model

Power turbine stator PTS and inlet guide vanes IGV mathematical models are almost the same except the parameters and dimentions of the electro-hydraulic servo acruator. They are different in the dimensions as bore diameter, rod diameter and stroke. To correctly simulate both systems response, too many parameters have been identified. Some of them were directly measured. Some other parameters had been estimated or assumed.

The mathematical model of the system has been built in three main parts according to the real system as following:
- Electro-magnetic proportional solenoid.
- Electro-hydraulic servo-proportional valve.
- Electro-hydraulic servo actuator.

Each subsystem is described by more than one set of differential equations. SIMULINK is used to simulate the

dynamic response of system. Because of intention to run the model on a real time target, it was configured for fixed step Simulink solver. ODE3 (Bogacki-Shampine) continuous explicit solver with step size of (1E-5 s) was used to solve the model.

1- Electro-magnetic proportional solenoid:

The solenoid can be represented as a linear inductor (L) with a resistor in series (R) as shown in figure 6.
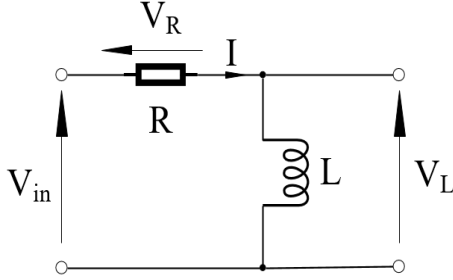

Fig. 6. Electro-magnetic proportional solenoid equivalent circuit

The voltage/current relationship can be derived by:

$$V_i = V_R + V_L = iR + L\frac{di}{dt} + i\frac{dL}{dt} \qquad (1)$$

For too small displacement (less than 1 mm each side) the inductance rate of change is tiny so it can be neglected. The new equation will be:

$$V_i = iR + L\frac{di}{dt} \qquad (2)$$

The current force relationship can be described as a linear equation between the magnetic force affecting the solenoid core and the current passing through its coil. The proportionality factor $k_s i$ is the current force gain, N/A.

$$F_M = k_{si} * i \qquad (3)$$

In other hand the mechanical behavior of the solenoid can be described by a spring damped mass system. According to Newton's 2nd law the equation of motion of the system is:

$$m_c x_c'' = F_M + F_p + F_{seat} - W_c - k_c(x_c + x_{c0}) - f_c x_c' - F_{Gap} \qquad (4)$$

Where : m_c is the solenoid moving parts mass in kg, x_c is the solenoid core displacement in m, F_M is the magnetic force affecting the solenoid core in N, F_P is the pressure force affecting solenoid core in N, F_seat is the seat reaction force in N, W_c is the solenoid moving parts weight in N, K_c is the solenoid spring stiffness in N/m, f_c is the solenoid damping coefficient in N.s/m, x_{c0} is the solenoid spring initial compression in m, F_{Gap}

is the seat reaction between spool and core in N

The pressurized fuel coming out of the amplifier nozzle affects the solenoid core by a force (F_p) which can be described by equation:

$$F_p = P_v A_{sc} = P_v * \frac{\pi}{4} d_{sc}^2 \qquad (5)$$

$$F_{seat} = \begin{cases} 0 & x_c > 0 \\ k_{seat} * |x_c| + f_{seat} * |x_c'| & x_c \leq 0 \end{cases} \qquad (6)$$

Where : P_v is the spool amplifier pressure in Pa, A_{sc} is the solenoid core's area presented to spool's nozzle flow in m^2, k_{seat} is the seat equivalent stiffness in N/m, f_{seat} is the seat equivalent damping coefficient in N.s/m.
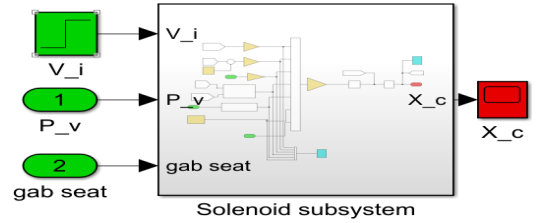

Fig. 7. Electro-magnetic proportional solenoid model

2- Electro-hydraulic servo-proportional valve:

*Amplifier flow equations:

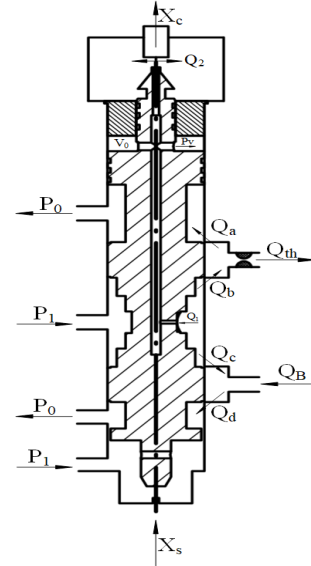$$Q_1 = C_d A_1 \sqrt{\frac{2}{\rho}(P_1 - P_v)} \quad Q_2 = C_d A_1 \sqrt{\frac{2}{\rho}(P_v - P_0)} \qquad (7)$$

Fig. 8. Electro-hydraulic servo-proportional valve

One of the two areas is constant (A_1), while the other (A_n) depends on the gap as follows:

$$A_1 = \frac{\pi}{4}d_1^2 \qquad (8)$$

$$gap = (x_i + x_c - x_s) \qquad (9)$$

Where : Q_1 is the flow rate through hydraulic amplifier inlet port in m^3/s, Q_2 is the flow rate through hydraulic amplifier variable nozzle in m^3/s, A_1 is hydraulic amplifier inlet port area in m^2, A_n is hydraulic amplifier variable nozzle area in m^2, P_1 is the valve supply pressure in Pa, P_0 is the valve return pressure in Pa, ρ is the fuel density in kg/m^3, C_d is the discharge coefficient, x_i is the initial distance between spool and solenoid core in m, x_s is the spool displacement in m.

*Amplifier continuity equations:

$$Q_1 - Q_2 + A_s\frac{dx_s}{dt} = \frac{V_0 - A_s x_s}{B}\frac{dP_v}{dt} \qquad (10)$$

$$A_s = \frac{\pi}{4}(D_s^2 - D_a^2) \qquad (11)$$

Where : A_s is the valve spool cross sectional area in m^2, V_0 is the valve initial volume in m^3, B is Bulk's modulus in Pa, x_s is the spool displacement in m.

* Equation of motion for the spool:

The motion of the spool is governed by the following equation of motion, neglecting the static friction force:

$$m_s x_s'' = P_1 A_r - P_v*(A_s+A_2) - f_s x_s' - F_{sseat} - F_j - W_s + F_{Gap} \qquad (12)$$

The spool displacement is limited mechanically by a limiter at the end of its stroke on both sides. When reaching any of the side limiters the seat reaction develops a counter force, F_{sseat}:

$$F_{sseat} = \begin{cases} k_{seat} - (x_s - x_{smin}) + f_{seat} - x_s' & \mathrm{x}_s \leq x_{smin} \\ 0 & \mathrm{x}_{smin} < x < x_{smax} \\ k_{seat} - (x_s - x_{smax}) + f_{seat} - x_s' & \mathrm{x}_s \geq x_{smax} \end{cases} \qquad (13)$$

As a result of fluid flow, a force, F_j , equal to the rate of change of the momentum of the fluid is generated. The momentum force directs all the time to close the valve port opening. It acts as a centering spring, and will be described here in by jet reaction force.

$$F_j = \begin{cases} \frac{\rho*Q_b^2}{C_c A_b} + \frac{\rho*Q_d^2}{C_c A_d} & \mathrm{x}_s > 0 \\ \frac{\rho*Q_a^2}{C_c A_a} + \frac{\rho*Q_c^2}{C_c A_c} & \mathrm{x}_s > 0 \end{cases} \qquad (14)$$

Where : m_s is the valve spool's mass in kg, A_r is valve's rear cap cross sectional area in m^2, A_2 is the nozzle

bore area in m^2, f_s is the spool damping coefficient in Ns/m, F_j is the jet reaction force in N, F_{sseat} is the spool's seat reaction force in N, W_s = spool's wieght in N, x_{smin} is the minimum spool displacement limit in m, x_{smax} is the maximum spool displacement limit in m, C_c is the contraction coefficient, Q_a, Q_b, Q_c, Q_d are the flow rate through ports openings (a, b, c, d) consequently in m^3/s, A_a, A_b, A_c, A_d are the areas of ports openings (a, b, c, d) consequently in m^2.

* Flow rates through the valve restriction areas:

The valve restriction areas, incorporated in this valve, are to be classified into sharp edged orifices and short tube orifice. Sharp-edged orifices are preferred because of their predictable characteristics. The pressure and power losses in these orifices are dominated by the fluid inertia. The fluid viscosity has no significant effect on their operation.

Therefore, the flow rate through sharp-edged orifices is viscosity-independent. On the other hand, for economy reasons, short tube orifice is used here as fixed restrictors in the flow passages. The fluid flow through a short tube orifice is subjected to the friction losses as well as the minor losses at inlet and outlet.

Therefore, these orifices are viscosity- dependent. The orifices caused by the spool displacement between the spool and the sleeve port's outlet are, due to the geometry, sharp edged orifices (a, b, c, d). The throttling orifice in the valve outlet is a short tube orifice. Neglecting the losses through the transmission lines which connect the valve to the actuator. The flow rates through the valve restriction areas are given by:

$$Q_a = C_d A_a\sqrt{\frac{2}{\rho}(P_x - P_0)} \qquad (15)$$

$$Q_b = C_d A_b\sqrt{\frac{2}{\rho}(P_1 - P_x)} \qquad (16)$$

$$Q_a = C_d A_c\sqrt{\frac{2}{\rho}(P_1 - P_B)} \qquad (17)$$

$$Q_a = C_d A_d\sqrt{\frac{2}{\rho}(P_B - P_0)} \qquad (18)$$

$$Q_a = C_d A_t h\sqrt{\frac{2}{\rho}(P_x - P_A)} \qquad (19)$$

The discharge coefficient, C_d, depends mainly on the contraction coefficient, C_c, and the orifice geometry. For a sharp-edged orifice, if the orifice diameter is much less than the pipe diameter, the discharge coefficient can be calculated using the following expression[4]:

$$C_d = C_c = \frac{\pi}{\pi + 2} = 0.611 \qquad (20)$$

The areas corresponding to the spool displacement can be classified into radial clearance area and port opening area. The port opening area can be described by the area of the segment corresponding to spool movement over the circular port of the valve multiplied by number of ports for each outlet.

$$A_{a,b,c,d} = \begin{cases} A_a = A_c = A_{rc} = \pi(D_s + c)c & x_s > 0 \\ A_b = A_d = A_{xs} + A_{rc} & x_s > 0 \end{cases} \qquad (21)$$

$$A_{a,b,c,d} = \begin{cases} A_a = A_c = A_{xs} + A_{rc} & x_s < 0 \\ A_b = A_d = A_{rc} & x_s < 0 \end{cases} \qquad (22)$$
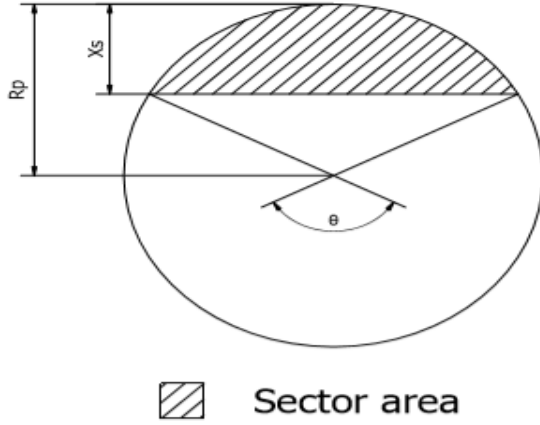

Fig. 9. Description of valve opening area calculation

$$A_{xs} = 4 * Axs_p \qquad (23)$$

$$A_{xs} = \frac{1}{2}r_p^2 * (\theta - Sin\theta) \qquad (24)$$

$$\theta = \arccos(\frac{r_p - |x_s|}{r_p}) \qquad (25)$$

$$A_{th} = \frac{\pi}{4} * d_{th}^2 \qquad (26)$$

Where : P_x is the pressure between port opening and throttle orifice in Pa, P_A is the pressure on the cap side of the actuator in Pa, P_B is the pressure on the rod side of the actuator in Pa, A_{th} is the throttle orifice area in m^2, A_{rc} is the radial clearance area in m^2, A_{xs} is the area of all ports opening due to spool displacement in m^2, A_{xs_p} is the area of single port opening due to spool displacement in m^2, r_p is the port radius in m.

* Continuity equation on the valve outlet:
By applying the continuity equation on the valve outlet neglecting the external leakage:

$$Q_b - Q_a - Q_{th} = \frac{V_x}{B}\frac{dP_x}{dt} \qquad (27)$$

$$Q_c - Q_d - Q_b = 0 \qquad (28)$$

Where : V_x is the volume between port opening and throttle orifice in m^3, Q_B is the flow rate at valve outlet on the rod side of actuator in m^3/s.
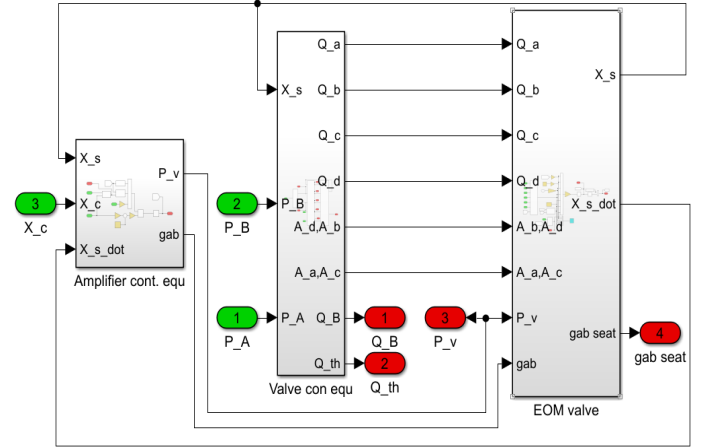
Fig. 10. Electro-magnetic proportional solenoid model

3- Electro-hydraulic servo actuator:

* Continuity equations of the cylinder chamber:

Applying the continuity equation to the cylinder chamber considering the internal leakage and neglecting the external leakage:

$$A_b\frac{dY}{dt} + \frac{P_A - P_B}{R_t} - Q_B = \frac{V_B - A_B * Y}{B}\frac{dP_B}{dt} \qquad (29)$$

$$Q_{th} - A_A\frac{dY}{dt} - \frac{P_A - P_B}{R_t} = \frac{V_A - A_A * Y}{B}\frac{dP_A}{dt} \qquad (30)$$

$$A_A = \frac{\pi}{4} * D_A^2 \qquad (31)$$

$$A_B = \frac{\pi}{4} * (D_A^2 - D_B^2) \qquad (32)$$

Where : Y is the actuator displacement in m, R_i is the resistance to internal leakage in actuator in N.s/m^5, V_A is the actuator cap side initial volume in m^3, V_B is the actuator rod side initial volume in m^3, A_A is the piston cap side area in m^2, A_B is the piston rod side area in m^2

* Equation of motion of the piston:

The motion of the piston under the action of pressure difference, viscous friction, inertia, external forces, and its own weight was described by the equation of motion. also the seat reaction force due to mechanical limitation was taken into consideration. The limiter force was described by an equivalent spring and damper reacting only when the piston reaches its limits:

$$m_p Y'' = P_A A_A - P_B A_B - f_p Y' - FAseat - F_{Load} + W_p \tag{33}$$

$$F_{Aseat} = \begin{cases} k_{seat} * Y + f_{seat} * Y' & Y \leq 0 \\ 0 & 0 < Y < Y_{max} \\ k_{seat} * (Y - Y_{max}) + f_{seat} * Y' & Y \geq Y_{max} \end{cases} \tag{34}$$

Where : m_p is the piston mass in kg, f_p is the actuator damping coefficient in Ns/m, F_{Aseat} is the actuator seat reaction force in N, F_{load} is the load force in N, W_p is the piston's weight in N, Y_{max} is the piston's stroke in m.
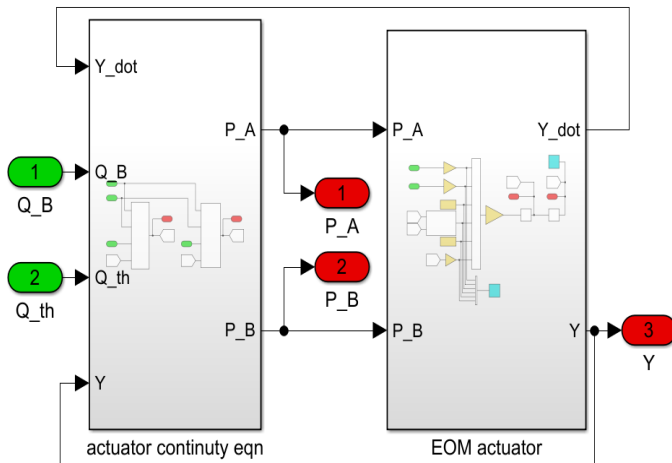

Fig. 11.   Electro-hydraulic servo actuator model

4- PTS total system:
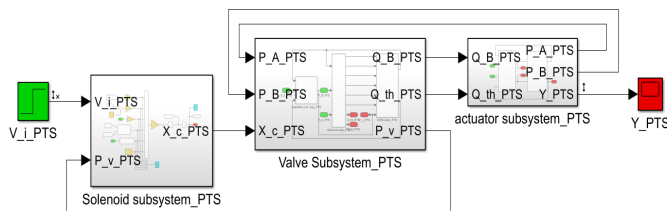
Fig. 12.   PTS total system

C. FM subsystem model

Measuring the parameters for the system under study, like the internal dimensions of these system components is very hard because of the system complicity and integrity. In this case it is preferred to treat the system as a black box.

The system identification is performed using Matlab's SIT by many researchers in different fields ([5], [6] and [7]). The toolbox has a useful graphical user interface (GUI) which is used to import the time domain data. The toolbox is used in another thesis[8] to estimate time continuous transfer function from this imported data.

The pound per hour (PPH) unit has been used in the engine manufacturer technical manual. So, in this study this unit has been chosen for the output mass flow rate representation to make the comparison process between the manufacturer FMS specifications and the study results more easily. The multiplication factor between the voltage representation and the PPH representation of the mass flow rate has been determined by measuring the output mass flow rate.at different points. The measurements show that converting the voltage representation of the mass flow rate to pound per hour (PPH) is achieved by multiplying the voltage value by 100.

$$G(s) = \frac{5.245S^3 + 106.1S^2 - 4.232S + 10.4}{S^4 + 10.6S^3 + 54.1S^2 - 1.147S + 4.644} \tag{35}$$

Fig. 13.   FM total system

D. EMFS total model

Fig. 14.   EMFS total system

V. Exprimental work

A. Test rig

-Test rig setup

Fig. 15.   Constructed test rig

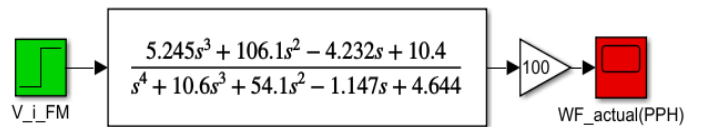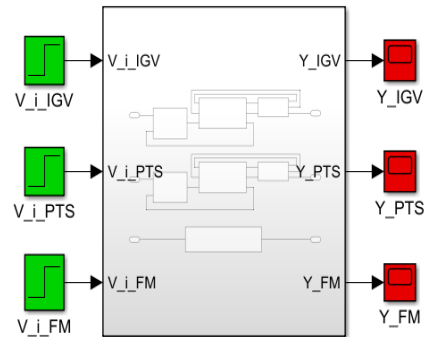For the experimental tests, a test rig is designed and constructed to be used as a demonstration for the engine's fuel management system and to test and validate the mathematical model of the system and to take measurements necessary to indicate engine performance and state.

The constructed test rig, as shown in Figure15, consists of a working bench holds the whole system's components together,most of these components are identical parts used in AGT1500 gas turbine engine and rest of components were either designed or manufactured to enable system running at a rotational speed different from the engine's idling speed to its maximum working speed.

The designed test rig is typically simulating the operation conditions of the original equipment, which strongly needed to discover the knowhow technology of the system. Also, the test rig is tunable in order to integrate the proper control system after investigating the system.

As demonstrated in the figure the test rig consists of two main sections: The first section is laying underneath the test rig bench, containing:

- fuel tank (100 liter).
- power lever actuator (PLA).
- power supply (2*12V).
- electrical control system.
- pump drive system (motor, belt mechanism, speed inverter and speed pickup system).

The second section is the one above the bench and contains:

- whole hydraulic system.
- control panel.
- control box.

-Test rig operation

Fig. 16.   Test rig block diagram

An AC (220 V) power supply is used as the main power source of the test rig, this high AC voltage transforms to DC voltage with different voltage values through the power supply (24DCV, 12DCV, -12DCV, 5DCV, 3.3DCV) with different functions, they are used to:

- Drive the electrical fuel pump.
- Supply the proportional solenoids controlling hydraulic system with current necessary.
- Provide the ability to generate a sinusoidal wave necessary for using variable differential transformers to measure actuators displacement and the power lever actuator.
- Power the control panel.
- Provide the ability for digital controlling of system using microprocessor integrated circuits.

Test rig operation starts by switching the main power switch and fuel pump switch to (ON) position so power supply delivers DC voltage to an electrical network box responsible for the correct distribution of this voltage.

The electrical network box distributes power to a pilot relay that controls the activation of an AC inverter. This AC inverter is used for controlling the speed of the main pump driving motor. The electrical motor drives the main hydraulic pump through two pulleys and belt mechanism.

The electrical fuel pump pumps fuel through a coarse filter, a water fuel separator, and a fine filter to the main hydraulic pump. The main hydraulic pump delivers fuel to two identical electrohydraulic valves IGV and PTS and a proportional solenoid fuel metering valve.

The test rig is provided with a main control box, a data acquisition card, a workstation, a human interface monitor, and an external power supply.

The main control box is controlling the whole test rig according to the power lever actuator request and collecting signals of the sensors and transmitters by means of branched wiring harnesses designed and manufactured specially for this purpose. The data acquisition card is connected to the main control box through a wiring cable transfers signals between both of them. Finally, data

acquisition card collects all measured, control, and feedback signals then sends them to the workstation through a data connection. An interface program was designed using LabVIEW software for monitoring, logging, and re-rendering the measured signals from the test rig. At the same time the control box sends these data to the control panel which present it to the user.

B. Measurements

To have an accurate mathematical mode, the physical parameters need to be measured. these parameters are the geometrical dimensions, the weight of the moving components, the coefficients of the materials in contact with each other, or the hydraulic fluid characteristics.

In order to measure the required tiny dimensions , an accurate measurement method is needed, a microscope set with 2 micrometers are used to measure the diameter of narrow holes that no gauge can measure them. Every dimension is measured in 10 iterations and the standard deviation is calculated to ensure accurate measurement.

Fig. 17.   Measurement process

C. Aquisition

Experimental measurements are necessary to understand the system behavior in several operation conditions which is essential for the modeling process. The measurement is done using different sensors and transducers (RVDT, LVDT, Speed pickup.... etc.). Acquisition system has been used for this purpose. It consists of three main parts; conditioning circuits, NI USB DAQ and LabVIEW (version 14.0.1) graphical user interface (GUI).

Conditioning circuits are necessary for current amplifications for driving of solenoids, for generating the required AC signal for LVDT primary coil excitation process and measure the output voltage of the secondary coil and finally for signal conditioning to make signals more suitable for measurement process.

Selection of Data Acquisition card depends on the number of channels required, resolution and mainly the

sampling rate and other parameters like precision and durability, all these parameters are necessary for monitoring, processing and logging of the coming data. For best performance, the minimum sampling rate is calculated based on the highest frequency of the measured signals which is the motor rotational speed measured using speed pickup. The maximum rotary speed of the motor is 4500 rpm and with each rotation the speed pickup read 29 signals so the minimum sampling rate necessary for proper measurement equals 2.1 KHz.

NI USB-6363 Card is chosen to acquire the measurement signals along with LabVIEW software platform to design a software program to process it. The LabVIEW Program is used to acquire, log and display the measured values and compare the results with the expected values.

The programing of this VI is divided into two main parts appears in two windows; the front panel window, and the block diagram window.

The front panel window is the user interface for the VI used to accomplish measurements displaying, or recording. It contains all the controllers and indicators of the program as well.
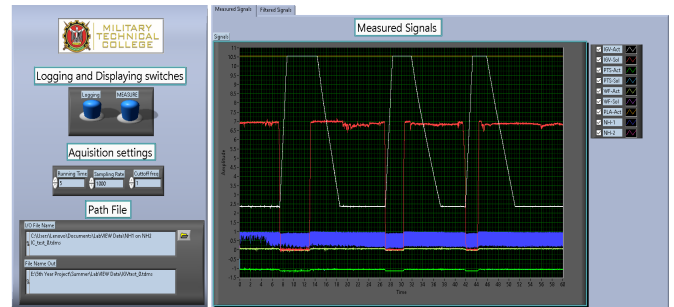

Fig. 18.   LabVIEW front panel

The block diagram section is the part containing the graphical source code of a LabVIEW program. The concept of the block diagram is to separate the graphical source code from the user interface in a logical manner. Front panel objects appear as terminals on the block diagram. Block diagram terminals reflect the changes made to their corresponding objects and vice versa.
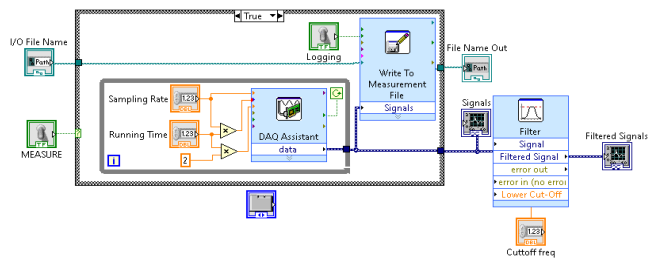

Fig. 19.   LabVIEW block diagram

VI. Results

A. IGV model results

1- Model response to null voltage input 5.5V:

It show the the response of the hydraulic actuator to input voltage at which it must be no movement in the closed loop.
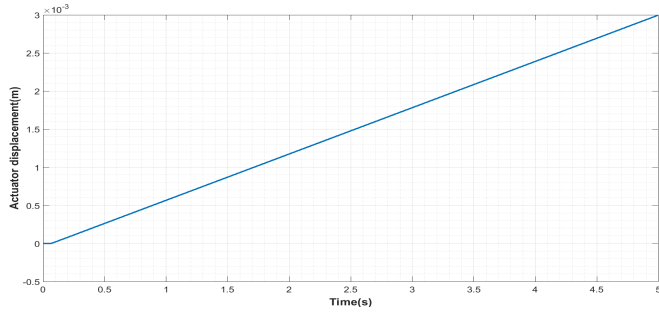

Fig. 20. IGV response to null voltage

2- Model response during extension stroke:

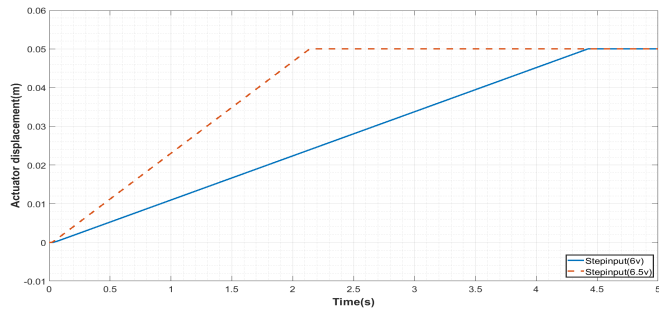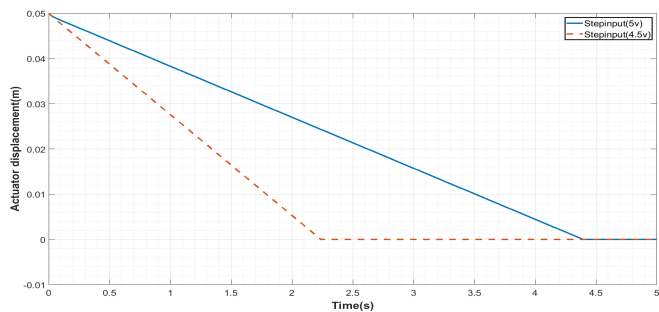It show the response of the hydraulic actuator according to two higher voltages than the null voltage.

Fig. 21. IGV response during extension stroke

3- Model response during retraction stroke:

It show the response of the hydraulic actuator according to two lower voltages than the null voltage.

Fig. 22. IGV response during retraction stroke

B. PTS model results

1- Model response to null voltage input 3.3V:

It show the the response of the hydraulic actuator to input voltage at which it must be no movement in the closed loop.

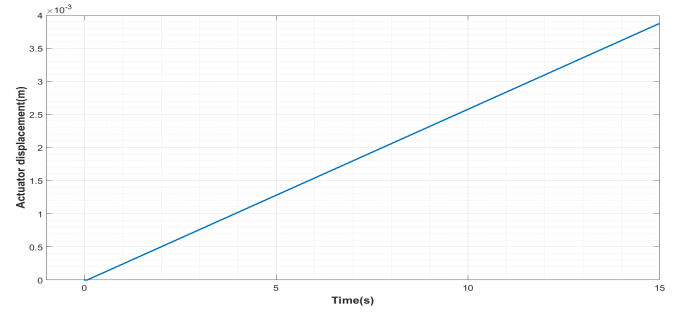The null voltage of PTS and IGV system is measured practically fron the test rig.

Fig. 23. PTS response to null voltage

2- Model response during extension stroke:

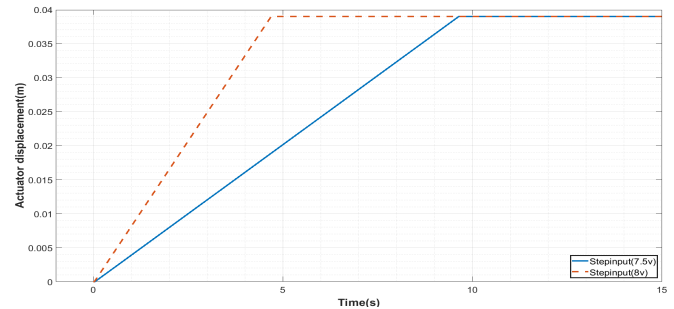It show the response of the hydraulic actuator according to two higher voltages than the null voltage.

Fig. 24. PTS response during extension stroke

3- Model response during retraction stroke:

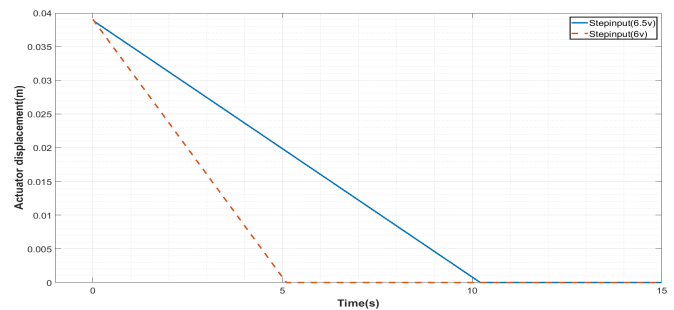It show the response of the hydraulic actuator according to two lower voltages than the null voltage.

Fig. 25. PTS response during retraction stroke

VII. Conclusion and future work

Accordingly, the mathematical dynamic model represented in this paper and it's simulation on SIMULINK can be considered as a verified model for the described system. Furthermore, it can be used to design and compare the effect of different control techniques on the system behavior for further development.

References

[1] S. J. Mohammadi, S. A. Miran Fashandi, S. Jafari, and T. Nikolaidis, "A scientometric analysis and critical review of gas turbine aero-engines control: From whittle engine to more-electric propulsion," Measurement and Control, vol. 54, no. 5-6, pp. 935–966, 2021.

[2] Roboteam, "Mtgr." http://www.roboteam.com/products/mtgr/s-2, 2017. Retrieved: August 2, 2022.

[3] M. M. Samy, M. A. Metwally, W. M. Elmayyah, and I. A. Elsherif, "Investigation of electrohydraulic control of a gas turbine engine's inlet guide vanes," in International Conference on Aerospace Sciences and Aviation Technology, vol. 17, pp. 1–10, The Military Technical College, 2017.

[4] M. G. El-Din and M. Rabi, Fluid power engineering. McGraw-Hill Education, 2009.

[5] F. Wang, C. Liang, Y. Tian, X. Zhao, and D. Zhang, "Design and control of a compliant microgripper with a large amplification ratio for high-speed micro manipulation," IEEE/ASME Transactions on Mechatronics, vol. 21, no. 3, pp. 1262–1271, 2016.

[6] R. Adnan, M. H. F. Rahiman, et al., "Model identification and controller design for real-time control of hydraulic cylinder," in 2010 6th International Colloquium on Signal Processing & its Applications, pp. 1–4, IEEE, 2010.

[7] T. Ling, M. Rahmat, A. Husain, and R. Ghazali, "System identification of electro-hydraulic actuator servo system," in 2011 4th International Conference on Mechatronics (ICOM), pp. 1–7, IEEE, 2011.

[8] M. Fadel, M. Metwally, W. Elmayyah, and I. Elsherif, "Black-box modelling of gas turbine engine's electrohydraulic fuel metering system.," in IOP Conference Series: Materials Science and Engineering, vol. 610, p. 012051, IOP Publishing, 2019.